



4-(4-Aminophenoxy)benzene-1,3-diamine-based covalent cross-linked sulfonated polyimide as proton exchange membranes in fuel cell

Gulshan Dhra¹ & Tharanikkarasu Kannan^{*2}

¹Department of Chemistry, University of Delhi, North Campus, Delhi 110 007, India.

²Department of Chemistry, Pondicherry University, R. V. Nagar, Kalapet, Puducherry 605 014, India.

E-mail: tharani.che@pondiuni.edu.in

Received: 30 June 2021; accepted 01 September 2021

Hydrolytic and oxidative stabilities of sulfonated polyimide membranes are of significant concern when they are used as fuel cell polyelectrolyte membranes. To increase the hydrolytic and oxidative stabilities of sulfonated polyimide membranes, a triamine crosslinker, 4-(4-aminophenoxy)benzene-1,3-diamine, was synthesized, characterized, and successfully used to synthesize covalently cross-linked sulfonated polyimide membranes. 1,4,5,8-Naphthalenetetracarboxylic dianhydride, 2,2'-benzidine-disulfonic acid, 4-(4-aminophenoxy)benzene-1,3-diamine and 2-bis(4-(4-aminophenoxy)phenyl)hexafluoropropane-based cross-linked sulfonated polyimide membranes have been synthesized and compared with linear sulfonated polyimide membrane in terms of various fuel cell application parameters. Covalent cross-linking is a simple and efficient method to increase the lifetime of the polyelectrolyte membranes. The covalently cross-linked sulfonated polyimide membranes show an ion exchange capacity of 1.426–1.441 meq.g⁻¹, proton conduction of 0.026–0.031 S cm⁻¹, and water uptake capacity 10.7–17.07%. As the triamine concentration is increased, both hydrolytic and oxidative stabilities of the membranes also increased. The linear sulfonated polyimide showed hydrolytic stability of 43 h, whereas hydrolytic stability of the cross-linked sulfonated polyimide membranes is increased up to 70 h.

Keywords: Covalent cross-linking, Fuel cell, Hydrolytic stability, Nafion[®], Oxidative stability, Proton conductivity, Polyelectrolyte membrane, Sulfonated polyimide

Fuel cells based on polymer electrolyte membranes have many advantages, and the most important one is their capacity to emit very low pollutants^{1,2}. Apart from these advantages, there are many challenges to construct an ideal fuel cell system that can give desired properties. Fuel cell membranes with better chemical and electrochemical stability are the main prerequisites for any membranes to act as polyelectrolyte membrane (PEM) in a fuel cell. In addition to this, good mechanical strength, higher proton conductivity, low fuel crossover, and low price are some of the essential focal points in fuel cell membrane research³. Nafion[®] and Flemion[®] membranes have been studied in detail and used as PEMs for fuel cells since the last decade as they have good process ability and better thermo-chemical stability⁴. Nafion[®], a perfluorosulfonated material-based membrane with a hydrophobic fluorocarbon-based backbone and hydrophilic sulfonic acid pendant side chain, has many advantages if used as a PEM in fuel cells. Due to this, it is being used as a polyelectrolyte membrane in practical polymer electrolyte membrane fuel cell (PEMFC) systems⁵. However, Nafion[®] has serious disadvantages such as higher fuel crossover⁶, lower proton conductivity, and lower water uptake

(WU) when the temperature is more than 80°C⁷. In addition, the manufacturing cost of Nafion[®] hampers its use in the practical PEMFC systems⁸. Hence, various types of alternative proton conducting membranes have been suggested for the last few decades⁹.

Sulfonated polyimide (SPI) membranes, due to their low fuel permeation, higher thermal stability, and good mechanical stability, have been considered as a promising candidate for this purpose by many research groups¹⁰⁻¹⁷. SPI membranes exhibit good film-forming capacity, which is an essential property for fuel cell applications^{18,19}. Moreover, the properties of polyimide membranes solely depend on the structures of the monomers. As a result, on changing the structure of the monomers, the properties of polyimides can also be altered considerably^{20,21}. Although SPI membranes have several good properties as a PEM candidate for PEMFCs, they have some severe disadvantages, such as less hydrolytic stability or water stability, which in turn disturbs their performance in fuel cell applications²². For instance, when the ion exchange capacity (IEC), a necessary property to offer proton conductivity, crosses the level of 2.0 meq.g⁻¹, the SPI membranes swell in water vapours and therefore show

low mechanical strength²². Furthermore, as the imide bond is prone to hydrolyse in higher water content and high temperature, polyimide undergoes depolymerisation at these conditions, and eventually, degradation of the polyimide backbone takes place²³. As a result, a considerable fall in the mechanical strength of the SPI membranes was observed under fuel cell operating conditions.

Hydrolytic stability and chemical structure of the SPI membranes are well related to each other, and some research groups have studied this relationship in detail. Okamoto has found that sulfonated diamines play a vital role in controlling the hydrolytic stability of the SPI membranes^{8,11-14,19,22,24}. The sulfonated diamines with more basic character produce SPI membranes with better hydrolytic stability than the weakly basic sulfonated diamines²⁵. To upgrade the mechanical and water stabilities of sulfonated polyimide membranes, various methods have been reported. Among these, ionic cross-linking of polyimide²⁵⁻²⁷ chains, preparing PEM with a low degree of sulfonation²⁸, using of a naphthalenic SPI in place of a phthalic SPI²⁹, preparing more hydrophilic-hydrophobic phase-separated polyimide³⁰, preparation of interpenetrating polymer networks³¹, introducing a flexible backbone^{12, 30, 32} in SPI membrane and covalent cross-linking in SPI membranes^{24,33,34} are some of the methods adopted. In the field of covalent cross-linking, many research groups have synthesized cross-linked sulfonated polyimides by using flexible aliphatic and aromatic triamine as a cross-linking agent and found that hydrolytic stability, oxidative stability, and mechanical stability of the cross-linked sulfonated polyimides have been improved immensely^{11,13,22,24,33,34}. Okamoto *et al.* used the post-polymerization method to prepare cross-linked sulfonated polyimide membrane with increased hydrolytic and oxidative stability^{22,24}. The sulfonic acid groups present in one linear polyimide chain were reacted with the activated hydrogen atoms of the aromatic rings of the other adjacent polyimide chains^{22,24}. Okamoto *et al.* also used triamine as a cross-linking agent to prepare covalently cross-linked sulfonated polyimide membranes to increase hydrolytic and oxidative stabilities^{13,33}. But, the triamine crosslinkers were added after the prepolymer formation stage. Due to this, the final sulfonated polyimide was either branched or cross-linked sulfonated polyimide membranes. But, Watanabe *et al.* used a triamine crosslinker along with the other dianhydride and

diamine monomers to get cross-linked sulfonated polyimide membranes³⁴. Surprisingly, the final product was initially precipitated in acetone and but, later on, dissolved in dimethylsulfoxide (DMSO) when the membranes were prepared.

In general, cross-linked polymers, once precipitated, does not dissolve again in any solvent. Therefore, it shows that the cross-linking density is less during the synthesis of polyimide membranes. In the present investigation, oxydibenzene-based flexible triamine cross-linking agent, 4-(4-aminophenoxy) benzene-1,3-diamine, 2 has been synthesized and used for the first time to prepare covalently cross-linked SPI(CCSPi) membranes with improved hydrolytic and oxidative stabilities with low membrane swelling. In addition, other important properties of the SPIs like proton conductivity, ion exchange capacity (IEC), thermal stability, and WU capacity have also been studied. Here, the triamine crosslinker was used along with the other monomers such as dianhydride, sulfonated diamine, and non-sulfonated diamine, using the procedure similar to the procedure followed by Watanabe *et al.*³⁴. But, it was attempted to check whether the cross-linked polyimide dissolves in any solvent after the formation of cross-linked sulfonated polyimide membranes. As covalent cross-linking is an efficient method for synthesizing polyimide membranes with improved hydrolytic and oxidative stabilities, more and more triamine crosslinkers must be explored. In this aspect, recently, we have used stilbene containing triamine as a crosslinker to improve hydrolytic and oxidative stability. In this study, for the first time, 4-(4-aminophenoxy)benzene-1,3-diamine is used as a triamine crosslinker to get the covalently cross-linked polyimide membranes.

Experimental Section

Materials

Ethylacetate and *m*-cresol were purchased from Spectrochem, India, and S.D Fine chemicals limited, India, respectively. Triethylamine (TEA), benzoic acid, anhydrous SnCl₂, *p*-nitrophenol, and 1-chloro-2,4-dinitrobenzene acetone were obtained from Sisco Research Laboratories, Mumbai, India. 1,4,5,8-Naphthalene tetracarboxylic dianhydride (NTCDA) was purchased from Sigma-Aldrich, USA. 2,2'-Benzidine-disulfonic acid (BDSA) and 2-bis(4-(4-aminophenoxy)phenyl)hexafluoropropane (HFBAPP) were procured from TCI, Japan. DMSO was purchased from Merck, India. NTCDA, BDSA, HFBAPP, and benzoic acid were purified by drying

under reduced pressure before use, and *m*-cresol, TEA, and ethylacetate were distilled under reduced pressure. Other chemicals were used without any further purification.

Synthesis of 2,4-dinitro-1-(4-nitrophenoxy)benzene, 1

To a 250 mL single-neck RB flask fitted out with a magnetic agitator, 2 mmol of *p*-nitrophenol and 3 mmol of anhydrous K_2CO_3 in 20 mL of dry acetone were added. After that, mmol of 1-chloro-2,4-dinitrobenzene was added. Then, the reaction was stirred at room temperature (25-30°C) under a nitrogen atmosphere for 24 h. After the reaction was over, the solvent of the reaction was removed by evaporation under a vacuum. The resulting solid was dissolved in dichloromethane for workup and washed by water 3-5 times to remove the traces of K_2CO_3 . The resulting organic layer was dried to remove moisture by anhydrous Na_2SO_4 and then concentrated. The resulting crude product, 1 was purified by column chromatography to obtain a dark brown to yellow coloured compound 1. Yield = 83 %. Proton NMR (400 MHz, $CDCl_3$): δ (ppm), 8.90 (s, 1H), 8.45 (d, 1H, $J=8.68$ Hz), 8.33 (d, 2H, $J=9.16$ Hz), 7.24 (d, 2H, $J=9.16$ Hz), 7.21 (d, 1H, $J=9.16$ Hz). IR (KBr, cm^{-1}): 3111 (Ar-C-H str), 1609 (Ar-C=C ring str) 1586 (Ar-C=C ring str), 1537 (-NO₂, asym.str), 1344 (-NO₂, sym.str), 1265 (Ar-C-O-C-Arstr). MS: *m/z*, 305.00. Elemental analysis: Theoretical calculation for $C_{12}H_7N_3O_7$: C (47.22%), H (2.31 %), N (13.77 %), O (36.70%). Experimental results: C (47.24 %), H (2.25 %), N (13.65 %), and O (36.86 %).

Synthesis of 4-(4-aminophenoxy)benzene-1,3-diamine, 2

To a 100 mL one-neck RB flask equipped with a magnetic stirrer and refluxing condenser, 0.25 mmol of 1 and 4.5 mmol of anhydrous $SnCl_2$ were dissolved in 15 mL of distilled ethanol, after that 5 mL of conc. hydrochloric acid was added. The resulting solution mixture was refluxed at 80°C under N_2 atmosphere for 4 h. After cooling the reaction mixture to 25-30°C, it was stirred overnight, followed by adding 1N NaOH solution to adjust the *pH* to about 8-9 to get the free amine. After standard workup with ethylacetate and dried with anhydrous Na_2SO_4 , the crude product, 2 was concentrated, dried, and purified by column chromatography. ¹H NMR (400 MHz, $CDCl_3$): δ (ppm), 6.77 (d, 2H, $J=8.8$ Hz, Ar), 6.66 (d, 1H, $J=8.08$ Hz, Ar), 6.62 (d, 2H, $J=8.8$ Hz, Ar), 6.16 (s, 1H, Ar), 6.05 (dd, 1H, $J=8.04$, 8.8 Hz, Ar), 4.87 (bs, 6H, NH_2). IR (KBr, cm^{-1}): 3447 (- NH_2 str.), 1634 (- NH_2 bend),

1508 (Ar-C=C ring str.), 1217 (Ar-C-O-C-Arstr.). MS: *m/z* 215.25. Elemental analysis: Theoretical percentage for $C_{12}H_{13}N_3O$: C (66.96 %), H (6.09 %), N (19.52 %), O (7.43 %). Experimental: C (67.98 %), H (6.84 %), N (17.85 %), and O (7.33 %).

Synthesis of linear SPI (sulfonated polyimide), LSPI

To synthesize LSPI, BDSA (0.5 mmol), *m*-cresol (5 mL), and triethylamine (1.2 mmol) were successfully charged into a 3-neck round bottom flask of 100 mL capacity under nitrogen atmosphere. First, BDSA was dissolved fully, then HFBAPP (0.5 mmol) was added to the flask and stirred until forming a homogeneous reaction mixture. To this solution, one mmol NTCDA and 1.5 mmol benzoic acid were also added. The reaction mixture was stirred at 25-30 °C for two minutes to reach a homogeneous solution. It was then stirred at 80°C for 4 h and at 180°C for 20 h in a nitrogen atmosphere. After a specified time, the reaction temperature was reduced to 120°C, and the syrupy solution obtained was transferred in dry CH_3COCH_3 with continuous stirring to attain a fibre-like precipitate. The fibre-like precipitate was first filtered off, washed many times with dry CH_3COCH_3 (acetone), and vacuum dried at 110°C for 10 h to obtain pure LSPI. The LSPI film was prepared by casting the DMSO solution (~ 5 wt %) of LSPI (triethylammonium salt form) onto a toughened glass plate by a spin coater. The spin-coated glass plates were preheated at 80°C for 1 h and dried up in a curing oven at 80°C, 120°C for 4 and 6 h respectively to evaporate the solvent. As-cast films were drenched in CH_3OH at 60°C for 1 h to eliminate the remaining DMSO. Proton exchange reaction was executed by dipping the films in 1.0 M HCl at 25-30 °C for 24 h. The resulting films were washed many times with deionized water and dried in a vacuum oven at 100°C for 20 h.

Synthesis of CCSPIs using 4-(4-aminophenoxy)benzene-1,3-diamine, 2

BDSA, *m*-cresol, and TEA were successfully charged into a 3-neck round bottom flask of 100 mL capacity in nitrogen current. First of all, BDSA was dissolved completely, then non-sulfonated diamine, HFBAPP, and triamine cross-linking agent 2 were added. To this solution, dianhydride, NTCDA, and C_6H_5-COOH were also added. The reaction was stirred at 25-30°C until the homogeneous reaction mixture was obtained. The homogeneous reaction mixture was heated with stirring at 80°C for 4 h and at

180°C for 20 h in a nitrogen atmosphere. After 24 h, the reaction temperature was reduced to 120°C, and the highly viscous polymer solution so obtained was cast onto a glass plate with the help of a spin coater to get the SPI films. The as-cast films (triethylammonium salt form) were dried in a curing oven at 120°C for 10 h. The dried films were immersed into CH₃OH at 60 °C for 1-2 h to eliminate the remaining solvent. Proton exchange was conducted by submerging the films in 1.0 molar concentration of HCl at 25-30°C for 24 h. The resulting films were washed with deionized water numerous times, followed by drying the films in a vacuum at 100°C for 20 h and more.

Measurements

Fourier-transform Nuclear magnetic resonance (FT-NMR) spectroscopy was used to record NMR spectra on Bruker DPX-300 NMR and 400 MHz NMR spectrometer JEOL-JNM-400P NMR instrument. Fourier-transform infrared (FT-IR) spectra were recorded by using a Nicolet Impact 400 FTIR instrument. Thermogravimetric analysis (TGA) was conducted by the thermogravimetric analyzer (TGA Q50 TA instrument, USA) applying 10°C/min heating rate in a nitrogen atmosphere. Differential scanning calorimetry (DSC) was carried out using the DSC Q200 instrument (TA instrument, USA) at a heating rate of 10°C/min in an N₂ atmosphere. The IEC of SPI films was measured by a well-known volumetric titration process. In this method, first, the sulfonated membranes were carefully washed with deionized water quite a few times, dried, and soaking in the 0.1 Molar NaCl solution for 18-20 h. The protons so released owing to the exchange with Na⁺ ions were finally titrated against 0.01 M NaOH solution by using phenolphthalein as an indicator. The IEC was calculated experimentally from the equation given below.

$$IEC \left(\frac{\text{mequiv}}{\text{g}} \right) = X \times \frac{N_{NaOH}}{\text{weight (polymer)}} \quad \dots (1)$$

Where the symbol X is the volume of the NaOH used and N_{NaOH} is the normality of the solution.

WU capacity measurement was carried out by dipping the proton exchanged films (0.2-0.3 g/sample) in the dry state in deionized water at 25-30°C for 20 h. Before immersion, the membranes in the dehydrated state were weighed using the microbalance. Then the films were taken out and spilled water was wiped out and weighed on a

microbalance quickly. Finally, WU capacity, S was calculated experimentally with the help of the following equation/formulae.

$$S (\%) = W_s - \frac{W_d}{W_d} \times 100 \quad \dots (2)$$

In the above equation, W_d and W_s are the weights of dry and wet membranes, respectively.

Proton conductivity of SPI membranes was determined by electrochemical impedance spectroscopic method in 100 kHz-10 Hz range. A square-shaped piece of SPI membrane in acid form and two pairs of platinum electrodes were adjusted into a Teflon cell followed by the placement of the cell in a thermo-controlled moist chamber for conductivity measurement at a lower than 100 % relative humidity (RH) or in deionized water for the measure in water. The proton conductivity (σ) was calculated using the given equation below.

$$\sigma \left(\frac{S}{cm} \right) = \frac{1}{\Omega} \times \frac{d}{A} \quad \dots (3)$$

In the above equation, 'd' is the distance between the platinum electrodes. A and Ω are the area and resistance of the SPI membranes, respectively. A known soaking and folding method was used to determine the hydrolytic stability of LSPI and CCSPI films. This soaking and folding involve immersing the membranes in hot water at 80°C with constant stirring. If the membranes were broken during this process or when membranes are bent, it is mentioned as breakable after folding it 3 or 4 times. This procedure of stirring the films/membranes in hot water nonstop till the films become completely brittle¹¹. Oxidative stability of SPI membranes was investigated by immersing membranes in Fenton's solution, which has the composition of 30 wt % of H₂O₂ and 30 ppm of FeSO₄ solution at 30°C and measuring the time taken from soaking to start to dissolve (t1), till the membranes were completely dissolved (t2).

Results and Discussion

The hydrolytic stability of SPI membranes is an important property that plays a significant role in the mechanical properties of the membranes during fuel cell applications. To increase the water stability of SPIs membranes, various types of cross-linking such as ionic cross-linking^{16,25-27}, interpenetrating polymer

networks³¹, and covalent cross-linking^{24,33,34} have been attempted. In a continuous effort to increase the hydrolytic stability of SPI membranes for a fuel cell application, recently, stilbene containing triamine covalent crosslinker was used³⁵. In the present investigation, 4-(4-aminophenoxy)benzene-1,3-diamine, **2** is used to prepare covalently cross-linked sulfonated polyimide (CCSPI) membranes. First, to study this, 4-(4-nitrophenoxy)benzene-1,3-diamine, **1** was synthesized as given in Scheme 1.

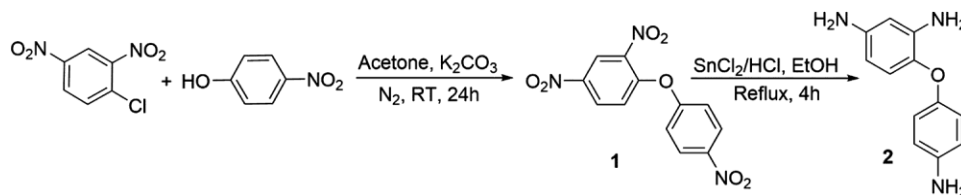
Synthesis of 4-(4-aminophenoxy)benzene-1,3-diamine, **2**

To prepare **2**, first, 4-hydroxynitrobenzene and 1-chloro-2,4-dinitrobenzene were reacted to get 2, 4-dinitro-1-(4-nitrophenoxy)benzene, **1**. The structure of **1** was confirmed by ¹H NMR, FT-IR, and mass spectroscopic techniques. In the ¹H NMR spectrum of **1**, no phenolic proton was observed, confirming the formation of compound **1**. The presence of a band at 1265cm⁻¹ is due to ether linkage (Ar-C-O-C-Ar) between the two aromatic rings and the absence of OH stretching vibrations of 4-hydroxynitrobenzene in the FT-IR spectrum confirm the formation of the compound **1**. The triamine **2** was synthesized from trinitro compound **1** as given in Scheme 1 by reducing **1** using anhydrous SnCl₂ and concentrated hydrochloric acid. The structure of **2** was confirmed

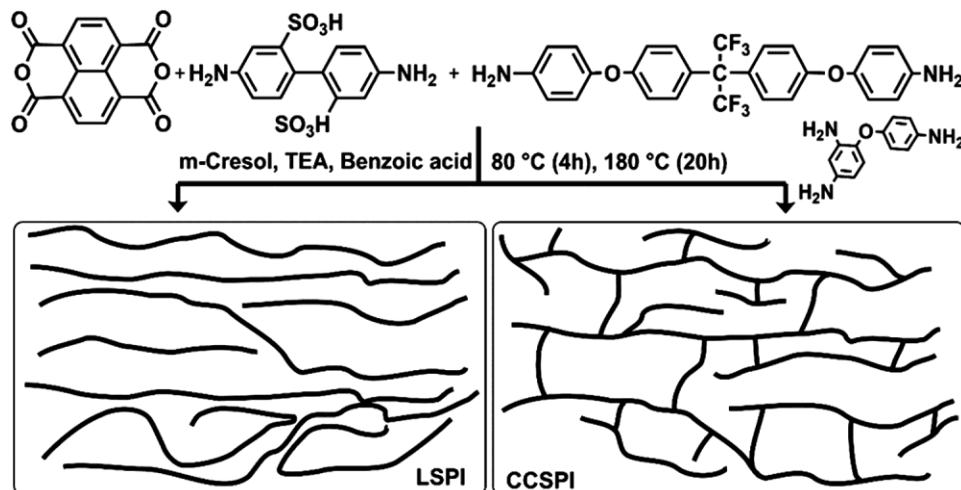
by NMR, FT-IR, and mass spectroscopic techniques. All the protons of compound **2** resonate at a higher field than its corresponding trinitro compound **1**. These results show that all three nitro groups have been converted into amino groups on reduction and confirm the formation of triamine **2**. In the Fourier Transform-infra red spectrum, the absorption band at 3447 cm⁻¹ is due to the stretching band of amino groups, and a band at 1634 cm⁻¹ is due to the bending vibration of -NH₂ groups. These results confirm that compound **2** was successfully synthesized from compound **1**. ¹H NMR and FT-IR spectra of compounds **1** and **2** are presented as supplementary data.

Synthesis of LSPI and CCSPI membranes

After successfully synthesizing the triamine **2**, it was used to synthesize CCSPIs as given in Scheme 2. To compare CCSPIs, linear SPI (LSPI) was also synthesized, as shown in Scheme 2. The chemical composition of different monomers used for the synthesis of LSPI and CCSPIs is given in Table 1. LSPI was prepared by one-step thermal condensation polymerization method¹⁸ using NTCDA as dianhydride, BDSA as a sulfonated diamine, and HFBAPP as non-sulfonated diamine as shown in Scheme 2. ¹H NMR spectroscopic method was used to confirm the chemical



Scheme 1 — Synthesis of triamine crosslinker, **2**.



Scheme 2 — Synthesis of CCSPI and LSPI.

Table 1—Synthesis of NTCDA-based linear and CCSPI membranes.

S. No.	Code	Nature ofSPI	NTCDA(mmol)	BDSA(mmol)	HFBAPP(mmol)	2(mmol)
1.	LSPI	Linear	2.0	1.0	1.0	0
2.	CCSPI-1	Crosslinked SPI	2.0	1.0	0.9993	0.000625
3.	CCSPI-2	Crosslinked SPI	2.0	1.0	0.9987	0.00125
4.	CCSPI-3	Crosslinked SPI	2.0	1.0	0.9975	0.0025
5.	CCSPI-4	Crosslinked SPI	2.0	1.0	0.9950	0.0050
6.	CCSPI-5	Crosslinked SPI	2.0	1.0	0.9900	0.0100

Reaction atmosphere: Benzoic acid = 3 mmol, TEA = 2.4 mmol, *m*-cresol = 8mL

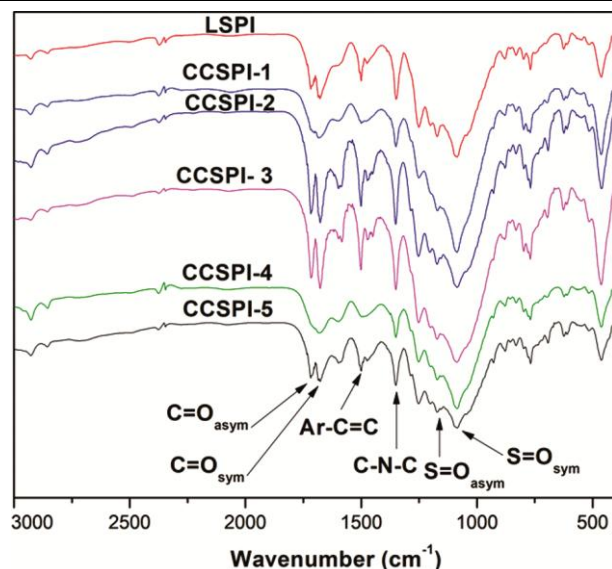


Fig. 1 — FT-IR spectra of CCSPI and LSPI.

structure of LSPI (cf. Supplementary data for ^1H NMR spectrum of LSPI). The integration ratio of diamine to naphthalenic protons was found to be in decent agreement with the structure of the resulting LSPI. Similar to LSPI synthesis, CCSPIs were also synthesized using the same method. But, during CCSPIs synthesis, as given in Scheme 2, compound 2 was also used in addition to the monomers used in LSPI synthesis. The mole ratio of different monomers used in the synthesis of CCSPIs is given in Table 1. As covalently cross-linked SPIs are generally brittle, it was very difficult to synthesize and prepare membrane out of them. When a higher concentration of cross linker was used during the synthesis than the concentration mentioned in Table 1, the resulting CCSPIs were highly viscous. The resulting CCSPIs could not be easily cast onto the glass plates afford the thoroughly homogeneous membranes of adequate thickness. Therefore, a very less mole ratio of the triamine crosslinker 2 has been used to get the good membranes of CCSPIs.

The CCSPI membranes could not be dissolved in any solvent, and hence, NMR spectroscopy could not

Table 2—Solubility of linear and CCSPI membranes

S. No.	Code	<i>m</i> -cresol	DMSO	DMF	NMP
1.	LSPI	+	+	±	±
2.	CCSPI-1	-	-	-	-
3.	CCSPI-2	-	-	-	-
4.	CCSPI-3	-	-	-	-
5.	CCSPI-4	-	-	-	-
6.	CCSPI-5	-	-	-	-

+ = Soluble; ± = Partially soluble; - = Insoluble

be used for the structural confirmation of CCSPI membranes. But, their chemical structure was confirmed by IR spectroscopy. Figure 1 shows the FT-IR spectra of LSPI and CCSPI membranes. The characteristic vibration of the carbonyl group of anhydride in NTCDA (1778 and 1737 cm^{-1}) is moved to some lower values as anhydride transformation to imide occurs. Therefore, the existence of characteristic absorption bands of $>\text{C}=\text{O}$ group of imide linkage at 1718 cm^{-1} (asymmetric) and 1677 cm^{-1} (symmetric) endorses the polyimide formation. The non-appearance of an IR absorption band corresponds to polyamic acid nearby 1780 cm^{-1} supports the complete conversion of polyamic acid to polyimide. The $\text{O}=\text{S}=\text{O}$ vibrations of the $-\text{SO}_3\text{H}$ group are observed at 1172 cm^{-1} and 1085 cm^{-1} as broadbands. The distinctive imide ring linkage $\text{C}-\text{N}-\text{C}$ is seen at 1348 cm^{-1} . There is no considerable difference between FT-IR spectra of LSPI and CCSPI membranes as the concentration of the crosslinker 2 is significantly less. But, solubility test results for CCSPI membranes, as given in Table 2, show that the cross-linked sulfonated polyimides are not soluble in any organic solvents. But, LSPI was soluble appreciably in high boiling aprotic solvents like, dimethylsulfoxide, *N*-methylpyrrolidine, dimethylformamide, and *m*-cresol. These results show that the crosslinker 2 was incorporated into the CCSPI membranes and formed a three-dimensional network structure as given in Scheme 2.

IEC, WU capacity and proton conductivity

After successfully synthesizing LSPI and CCSPI membranes, they were characterized for their fuel cell

suitability. IEC is an important property, and proton conductivity and WU depend on the ion exchange capacity of the SPI films/membranes. Therefore, it gives an idea of the actual ion-exchange sites existing for the conduction of protons in the SPI membranes under fuel cell operational conditions. IEC is determined by a recognized volumetric titration procedure. It has been witnessed that enhanced IEC values commonly display the more excellent proton conductivity, but SPI with a higher IEC value is lower in its hydrolytic strength. In the present investigation, the equal molar concentration of the sulfonated diamine was used to synthesize LSPI and CCSPI membranes. Hence, the ionic content of all LSPI and CCSPI membranes is the same, and the results are given in Table 3. Water uptake is an essential property of the SPI membranes in a fuel cell. In common, WU capacity is directly proportional to the proton conductivity. It is attributed to the fact that more WU imparts more ionic content and eventually leads to higher proton conductivity.

Generally, WU is influenced by the IEC values or $-SO_3H$ content existing in the polymer. The results of the WU capacity of LSPI and CCSPI are given in Table 3. As the concentration of 2 increases, WU capacity decreases. It is due to the reason that the cross-linking increases the rigidity of the main backbone of the SPI membranes, and rigidity inhibits the water penetration into the membranes. Therefore, it leads to less WU

capacity values as the crosslinker concentration increases. The proton conductivities of cross-linked sulfonated polyimides along with the linear SPI membranes and Nafion[®] 117 are given in Table 3. The cross-linked SPI membranes show slightly less conductivity than linear sulfonated polyimide membrane. Lower proton conductivities of CCSPI membranes are due to the lower WU uptake capacity of CCSPI membranes. However, both linear and cross-linked sulfonated polyimides show lower proton conductivity than the standard Nafion[®] 117 membrane.

Hydrolytic stability and oxidative stability

Hydrolytic stability and proton conductivity are the most important properties that decide SPI membrane-based fuel cell efficiency. SPI membranes show low hydrolytic stability than non-sulfonated polyimide membranes at hydrated conditions. In a hydrated state, OH nucleophile attacks the imide bond and, as a result, de-polymerization of polyimide chains takes place²⁸. During the degradation, the molecular weight of the polymer decreases, and the films become brittle and show reduced mechanical strength and durability¹⁸. To test the effect of covalent cross-linking in sulfonated polyimide membranes, in the present investigation, covalent crosslinker 2 was used to get CCSPI membranes. Hydrolytic stability data of the sulfonated polyimide membranes are given in Table 4. As the concentration of the crosslinker, 2, increases, hydrolytic

Table 3 — Ion Exchange capacity, Water uptake and Proton conductivity of SPI membranes.

S.No.	Code	Theoretical IECs (meq. g ⁻¹)	Experimental IECs (meq. g ⁻¹)	Water uptake* (%)	Proton conductivity* (S cm ⁻¹)
1.	LSPI	1.469	1.450	18.93	0.032
2.	CCSPI-1	1.469	1.432	17.07	0.031
3.	CCSPI-2	1.469	1.426	15.30	-
4.	CCSPI-3	1.469	1.435	13.07	0.026
5.	CCSPI-4	1.469	1.441	12.15	-
6.	CCSPI-5	1.469	1.428	10.70	-
7.	Nafion [®] 117	≥ 0.90	-	37.0	0.060

* At 30° C

Table 4 — Hydrolytic stability and oxidative stability of SPI membranes.

S. No.	Code	Hydrolytic stability		Oxidative stability		
		Temperature (°C)	Time taken to become brittle* (h)	Temperature (°C)	Time taken to dissolve** (h)	
					t ₁	t ₂
1.	LSPI	80	43	30	13	48
2.	CCSPI-1	80	46	30	14	52
3.	CCSPI-2	80	49	30	16	53
4.	CCSPI-3	80	58	30	16	55
5.	CCSPI-4	80	67	30	17	57
6.	CCSPI-5	80	70	30	18	61

*When the film has broken already or the films/membrane has broken upon folding 3-4 times, then it is brittle.

**When the membrane starts dissolving (t₁) and fully dissolved (t₂) are mentioned here.

stability also increases. It leads to the fact that the cross-linked network structure of the polymer allows reduced swelling of the SPI backbone. The hydrolytic stability of the LSPI is 43 h, whereas hydrolytic stability of the CCSPI membranes is increased up to 70 h with the addition of 0.01 mmol of the crosslinker 2.

Similarly, oxidative stability of the SPI membrane has also been found out by determining the time taken by the membranes when they started to dissolve (t_1) and fully dissolve (t_2) in Fenton's solution. Oxidative strength/stability outcomes are prearranged in Table 4. As the crosslinker 2 concentration increases, oxidative stability also increases. It is important to note that a non-sulfonated diamine monomer (HFBAPP) has hydrophobic $-CF_3$ groups, which keep the water molecules away from the main polyimide backbone and prevent the attack water molecules containing oxidative radical entity on imide bond. However, it is not very close to the imide linkage. The oxidative attack by OH^\bullet and OOH^\bullet radicals are electrophilic in nature, and it occurs most likely on the imide group of the polymer. Even if one imide bond is broken, the crosslinker helps hold the other backbone chain, leading to higher oxidative and hydrolytic stabilities. From the table, it may be concluded that all the cross-linked sulfonated polyimides show higher oxidative stabilities (t_2) than the oxidative stability of linear sulfonated polyimide membrane due to the formation of the cross-linked network.

Thermal properties

The glass transition temperature of polyimides is closely related to the chemical structure of the polyimides. The presence or absence of segmental and molecular motions determines whether a polymer is solid or rubbery, or in a molten state. In DSC analysis, the T_g of the LSPI membrane could not be visible clearly as more homogeneous phases are present in LSPI. But, a small hump is seen at $\sim 320^\circ\text{C}$. But, as given in Figure 2, as the crosslinker concentration was increased, the T_g of the cross-linked membranes started appearing. It may be because the segmental motions of the SPI chains are restricted due to the increase of the concentration of the crosslinker. The restricted movement of the SPI segments started forming phase separation, which in turn shows glass transition temperature. When 0.625 μmol of cross linker 2 is used (CCSPI-1), there are two T_g appeared at 320 and 340 $^\circ\text{C}$. But, these two T_g are very weak, and when the crosslinker concentration is increased to 1.25 μmol is used (CCSPI-2), the two T_g (318 and 340 $^\circ\text{C}$) are more

pronounced, and mainly the segment corresponds to higher temperature is more pronounced. When the crosslinker concentration is further increased to 2.5 μmol (CCSPI-3), the two phases are homogenized, and as a result, a single T_g is observed at 340 $^\circ\text{C}$. Further increase of the crosslinker concentration to 5 μmol (CCSPI-4) leads to forming two segments with the T_g at 322 and 351 $^\circ\text{C}$. Interestingly, further increase of the crosslinker concentration to 10 μmol (CCSPI-5) ends up with three humps at 320, 335 and 353 $^\circ\text{C}$. A further increase could not be studied due to the heterogenous formation of films. These results show that the crosslinker restricts the movements of SPI chains; due to this, phase separation also takes place.

The thermal stability of both LSPI and CCSPI membranes has been studied, and the results are presented in Fig. 3. Linear as well as cross-linked SPI

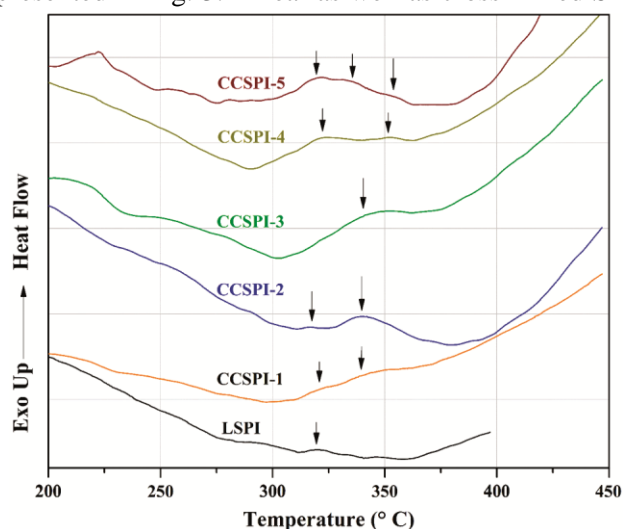


Fig. 2 — DSC curves of LSPI and CCSPI.

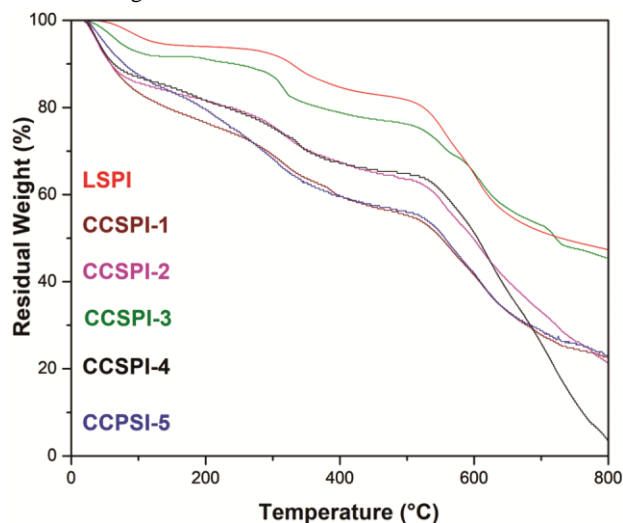


Fig. 3— TGA thermo grams of LSPI and CCSPI membranes.

membranes show a 3-step degradation array in TGA. The initial weight loss was witnessed at 100°C, owing to the loss of moisture absorbed by highly hygroscopic -SO₃H groups present in SPI membranes. The subsequent step is due to the degradation of the -SO₃H group, and it occurs around 230-350°C. And finally, the third and last degradation step corresponds to the disintegration of the polyimide core, generally taking place above 500°C. It has been observed from Fig. 3 that the order of the stabilities of cross-linked sulfonated polyimides follow the order: CCSPI-5 < CCSPI-3 < CCSPI-4 < LSPI < CCSPI-1 < CCSPI-2.

Three series of cross-linked sulfonated polyimides show poor thermal stability than linear SPIs. It can be explained on the basis of the presence of more concentration of triamine cross-linking agent, which has lesser thermal stability than the polyimide backbone/core main chain. But, the other two series of cross-linked sulfonated polyimides, CCSPI-1, and CCSPI-2 show higher thermal stabilities than the linear sulfonated polyimide membrane. It can be explained by the fact that in the case of CCSPI-1 and CCSPI-2, cross-linking agent concentration is low but cross-linking effect is more. Hence, these results show that cross-linked SPI membranes can be a good candidate as polymer electrolyte membranes, particularly CCSPI-1, and CCSPI-2 which show the highest thermal stabilities among the series.

Conclusion

In continuation to enhance the hydrolytic and oxidative stabilities of sulfonated polyimides, one-pot in-situ covalently cross-linked SPI membranes have been synthesized for proton exchange and for the fuel cell. In cross-linked SPIs, triamine cross-linking agent 2 based on oxydibenzene moiety has been used successfully with flexible ether linkage for good water uptake and comparable proton conductivity. The structure of the SPI membranes was confirmed by NMR and FTIR spectroscopic techniques and these membranes have been checked for their fuel cell suitability by considering their thermal stability, hydrolytic stability, IEC, water uptake, and proton conductivity, as these are some of the most important properties of a polymer electrolyte membrane to be used in a fuel cell. It is concluded that covalent cross-linked sulfonated membranes display higher hydrolytic and oxidative stabilities than the linear SPI membranes. Hence, these membranes could serve better candidates as polymer electrolyte membranes for fuel cell application without losing proton conductivity.

Acknowledgements

The author, Tharanikkarasu Kannan desires to thank University Grants Commission (UGC), New Delhi, for the financial support under the Special Assistance Program, stage DSA-I to Department of Chemistry, Pondicherry University (No. F.540/6/DSA-1/2016/(SAP-1) Dated 31-10-2018). Authors thanks Central Instrumentation Facility, Pondicherry University for characterization.

References

- 1 Kreuer K D, *J Memb Sci*, 185 (2001) 29.
- 2 Rikukawa M & Sanui K, *Prog Polym Sci*, 25 (2000) 1463.
- 3 Jones D J & Rozière J, *J Memb Sci*, 185 (2001) 41.
- 4 Odgaard M, *Elsevier*, (2015) 325.
- 5 Banerjee S & Curtin D E, *J Fluor Chem*, 125 (2004) 1211
- 6 Ahmed M & Dincer I, *Int J Energy Res*, 35 (2011) 1213.
- 7 Matos B R, Santiago E I & Fonseca F C, *Mater Renew Sustain Energy* 4 (2015) 16.
- 8 Hu Z, Yin Y & Chen S, *J Polym Sci Part A Polym Chem*, 44 (2006) 2862.
- 9 Peighambaroust S J, Rowshanzamir S & Amjadi M, *Int J Hydrogen Energy*, 35 (2010) 9349.
- 10 Besse S, Capron P & Diat O, *J New Mater Electrochem Syst*, 5 (2002) 109
- 11 Fang J, Guo X & Harada S, *Macromolecules*, 35 (2002) 9022.
- 12 Watari T, Fang J & Tanaka K, *J Memb Sci*, 230 (2004) 111.
- 13 Yin Y, Hayashi S & Yamada O, *Macromol Rapid Commun*, 26 (2005) 696.
- 14 Yamada O, Yin Y & Tanaka K, *Electrochim Acta*, 50 (2005) 2655.
- 15 Einsla B R, Kim Y S & Hickner M A, *J Memb Sci*, 255 (2005) 141.
- 16 Lee C, Sundar S, Kwon J & Han H, *J Polym Sci Part A Polym Chem*, 42 (2004) 3612.
- 17 Yin Y, Yamada O & Suto Y, *J Polym Sci Part A Polym Chem*, 43 (2005)
- 18 Genies C, Mercier R & Sillion B, *Polymer (Guildf)*, 42 (2001) 359.
- 19 Yin Y, Suto Y & Sakabe T, *Macromolecules*, 39 (2006) 1189.
- 20 Rehman W, Liaqat K & Fazil S, *J Polym Res*, 26 (2019) 82.
- 21 Srinate N, Thongyai S, Weiss R A & Praserttham P, *J Polym Res*, 20 (2013) 138.
- 22 Fang J, Zhai F & Guo X, *J Mater Chem*, 17 (2007) 1102.
- 23 Wei H, Chen G & Cao L, *J Mater Chem A*, 1 (2013) 10412.
- 24 Yaguchi K, Chen K & Endo N, *J Power Sources*, 195 (2010) 4676.
- 25 Kerres J A, *J Memb Sci*, 185 (2001) 3.
- 26 Jin R, Li Y & Xing W, *Polym Adv Technol*, 23 (2012) 31.
- 27 Sundar S, Jang W & Lee C, *J Polym Sci Part B Polym Phys*, 43 (2005) 2370.
- 28 Jang W, Lee C & Sundar S, *Polym Degrad Stab*, 90 (2005) 431.
- 29 Einsla B R, Hong Y T & Seung Kim Y, *J Polym Sci Part A Polym Chem*, 42 (2004) 862.
- 30 Seo J, Cho K Y & Han H, *Polym Degrad Stab*, 74 (2001) 133.

- 31 Lee S, Jang W & Choi S, *J Appl Polym Sci*, 104 (2007) 2965.
- 32 Guo X, Fang J & Tanaka K, *J Polym Sci Part A Polym Chem*, 42 (2004) 1432.
- 33 Yin Y, Yamada O & Hayashi S, *J Polym Sci Part A Polym Chem*, 44 (2006) 3751.
- Miyatake K, Asano N, Tombe T & Watanabe M , *Electrochem*, 75 (2007) 122.